JOURNAL OF GEOPHYSICAL RESEARCH, VOL. 86, NO. B7, PAGES 6067–6072, JULY 10, 1981

The Determination of Displacement Fields From Geodetic Data Along a Strike Slip Fault

WILLIAM H. PRESCOTT

U.S. Geological Survey, Menlo Park, California 94025
Stanford Rock Project, Department of Geophysics, Stanford University, Stanford, California 94305

Observations of angles or distances between stations of a geodetic network are commonly used to infer information about the movement of the surface of the earth. The absence of any observations external to the network leads to an ambiguous displacement field. Existing techniques for eliminating this ambiguity are all unsatisfactory in some respect. The best technique, an 'inner coordinate' solution, is not appropriate for networks located in a strike slip fault environment. The inner coordinate solution zeros the rotation of all stations about their center of mass. Along a strike slip fault like the San Andreas, however, motion normal to the fault is less likely than motion parallel to the fault. The solution presented here, an 'outer coordinate' solution, finds the rotation of the network that minimizes the components of displacement normal to the fault. Since motion along a strike slip fault is generally expected to be parallel to the fault, the displacements obtained with the outer coordinate solution are more reasonable than those obtained with other techniques. Examination of a trilateration network near San Francisco Bay demonstrates the large effect that the choice of adjustment technique can have on the inferred relative motion of the two sides of the fault. The inner coordinate solution gave a rate of about 1 mm/yr, whereas the preferred outer coordinate solution rate was 36 mm/yr.

INTRODUCTION

Repeated geodetic observations are frequently used to infer information about movement of the crust of the earth. The interesting parameters to be obtained from the data are usually the changes in station position, while the observations consist of measured angles and distances between the stations. The process of obtaining the station displacements from the observations is referred to as adjusting the data, and there is an extensive literature discussing the process of adjustment. Such an adjustment is a straightforward application of least squares techniques. If all observations are made between stations in the area of interest, there is no way to detect motion of all the stations as a rigid body. Consequently, the station displacements derived from the observations are ambiguous; the addition of an arbitrary translation or rotation will have no effect on the residuals to the observations resulting from the adjustment. The displacement ambiguity may be removed by making observations outside of the network. For example, the rotational ambiguity can be eliminated by observing one or more astronomic azimuths. The possible precision of such external observations is, at present, low in comparison to the possible precision of internal observations.

Without external observations only relative displacements are determined. Mathematically, the ambiguity expresses itself as a rank defect of 3 in the coefficient matrix of the normal equations. There are a number of solutions to this so called 'datum defect' [*Welsch,* 1979] problem. In this paper, I will review two popular solutions and derive a third solution, which is particularly appropriate when the tectonic setting of the area suggests that a particular azimuth may be preferred. Although in this paper the technique is applied only to trilateration networks (distances measured only), the methods apply without any alteration to triangulation or mixed triangulation-trilateration networks.

Paper number 1B0367.

ADJUSTMENT ALTERNATIVES

The issue is illustrated for a very simple network in Figure 1. Suppose for concreteness that all of the interstation distances are measured at each of two times and that the only change observed is that diagonal 1–3 lengthens and diagonal 2–4 shortens. Figure 2 illustrates a few of the possible solutions, and Figure 3 is a conventional vector displacement diagram for each of the solutions. All of these solutions are consistent with the lengthening of 1–3 and shortening of 2–4. They differ one from another only in rigid body motions of the four points. The traditional way to remove the datum defect has been to fix the position of two stations. This solution eliminates both translational and rotational ambiguities, but it can introduce some distortion in the network because the length of one line is constrained. In the past, when the observations were primarily angle measurements, this was the preferred solution. A second alternative is to fix one station and the azimuth of one line. This produces a 'free' adjustment, i.e., one with no unnecessary constraints. Examples are solutions in Figures 2*a*–2*c* and 3*a*–3*c*. There are two disadvantages to this approach. First, the displacements obtained depend on the azimuth of the fixed line, as illustrated by the comparison of solutions in Figures 2*a*–2*c* and 3*a*–3*c*. Second, displacements of all the stations depend on the motion of the two chosen stations. For example, if the fixed station was disturbed, a very large vector is added to all the other stations and this may obscure the smaller motions of the other stations relative to each other. Similarly, a large motion of the fixed azimuth station in a direction normal to the fixed line will introduce an apparent rotation of the whole network.

One solution to these problems, which has been much discussed recently is the 'inner coordinate' solution [*Brunner,* 1979; *Welsch,* 1979], illustrated by Figures 2*d* and 3*d*. For the inner coordinate solution the ambiguity is removed by requiring that the center of mass of the network be stationary and that there be no net rotation about the center of mass. In symbols, if x_k, y_k, u_k, v_k are respectively the position coordinates and displacement coordinates of the kth station, then the inner coordinate solution has the property that

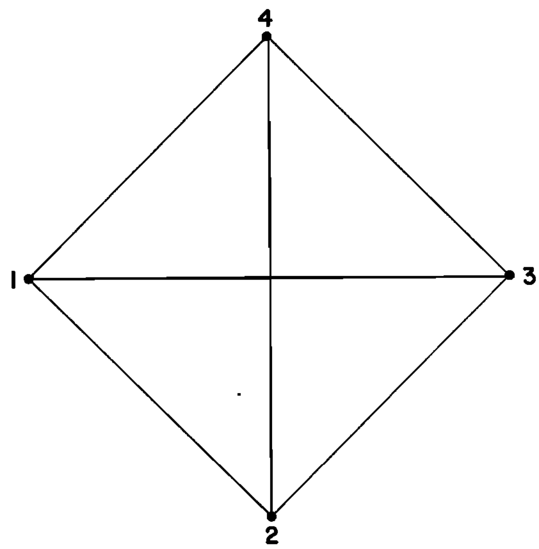

Fig. 1. A simple horizontal quadrilateral with all six lengths observed.

$$\sum u_k = \sum v_k = 0$$

$$\sum (x_k v_k - y_k u_k) \Big/ \sum (x_k^2 + y_k^2) = 0$$

The inner coordinate solution has the advantage of being only weakly dependent on any particular stations. The inner coordinate solution is the solution obtained if generalized inverse techniques are used in solving the normal equations. In the absence of any a priori knowledge of the deformation field it is an excellent choice.

Along the San Andreas fault system in California, however, there is an a priori expectation that station motion will most likely be along the direction of the faults and the relative plate motion N45° W approximately. The expected deformation is that shown in Figure 3*a*, for example, with right lateral shear across a line striking N45°W. The solution in Figure 3*d*, which differs from Figure 3*a* only by a rigid translation and

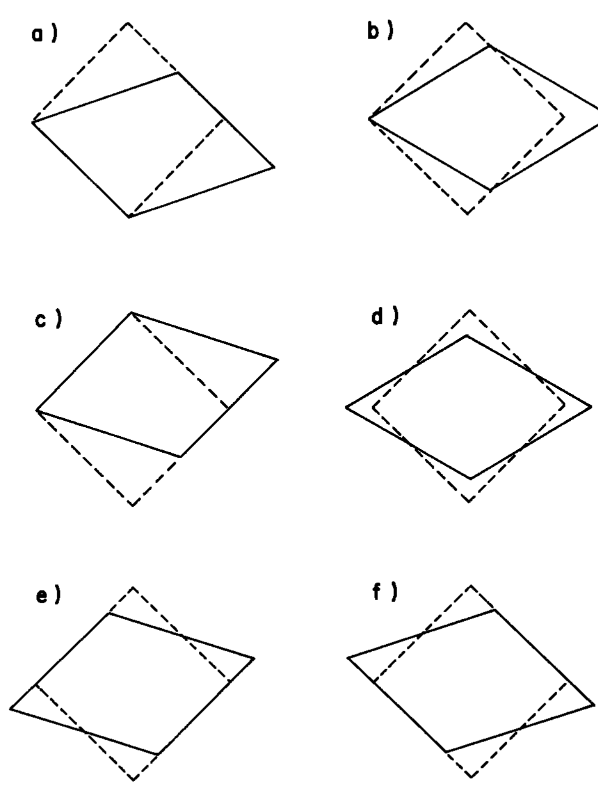

Fig. 2. Comparisons of initial (dashed lines) and final (solid lines) states of quadrilateral in Figure 1, assuming only observed changes are a lengthening of 1-3 and shortening of 2-4. North at the top of the figure (*a*) Corner 1 and the azimuth of the line 1-2 are fixed. (*b*) Corner 1 and the azimuth of line 1-3 are fixed. (*c*) Corner 1 and the azimuth of line 1-4 are fixed. (*d*) Inner coordinate adjustment. (*e*) Outer coordinate adjustment with the direction NE-SW preferred. (*f*) Outer coordinate adjustment with the direction NW-SE preferred.

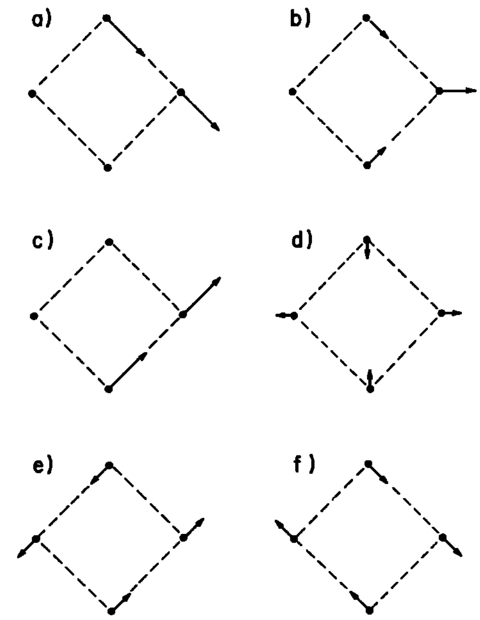

Fig. 3. Vector displacement diagrams. North at the top of the figure. (*a*) Corner 1 and the direction of line 1-2 are fixed. (*b*) Corner 1 and the direction of line 1-3 are fixed. (*c*) Corner 1 and the direction of line 1-4 are fixed. (*d*) Inner coordinate adjustment. (*e*) Outer coordinate adjustment with direction NE-SW preferred. (*f*) Outer coordinate adjustment with the direction NW-SE preferred.

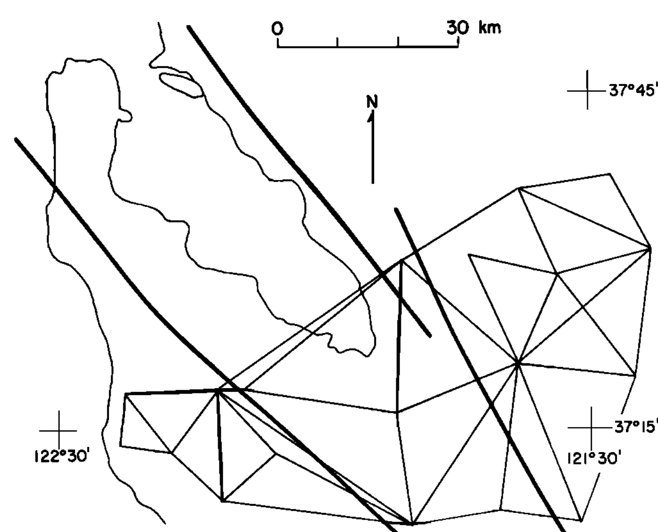

Fig. 4. Diagram of a trilateration network. Heavy lines represent the San Andreas, Hayward, and Calaveras faults. Light lines represent distances observed repeatedly between 1972 and 1979.

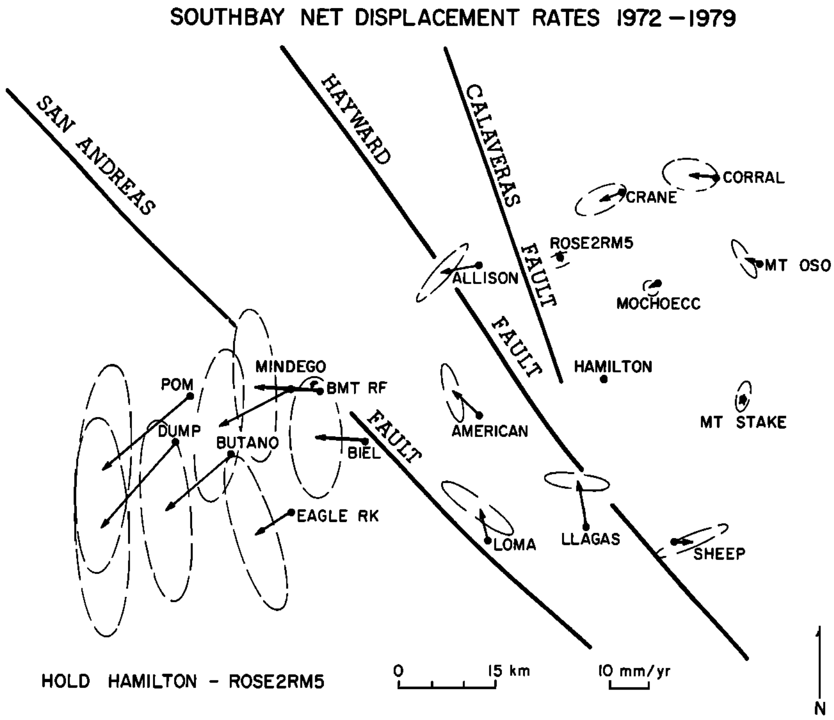

Fig. 5. Vector displacement diagram for a special solution. Station Hamilton and the azimuth of the line Hamilton-Rose2RM5 are fixed. Error ellipses are drawn at 95% confidence level.

rotation of the network, is clearly not the most transparent way of displaying the deformation. It is possible to have the advantage of favoring a particular direction without the disadvantage of having the whole solution dependent on one or two stations. Two examples are illustrated by the solutions in Figures 2*e*, 2*f*, 3*e*, and 3*f*. In the solution in Figures 2*e* and 3*e* the direction NE-SW is preferred and in the solution in Figures 2*f* and 3*f* the direction NW-SE is preferred. The solution in Figures 2*f* and 3*f* would be appropriate along the San Andreas fault system. These adjustments, which I have called outer coordinate solutions, are obtained by requiring that the center of mass of the network remain stationary and that the components of displacement normal to the preferred direction are minimized. The inner coordinate solution in Figures 2*d*

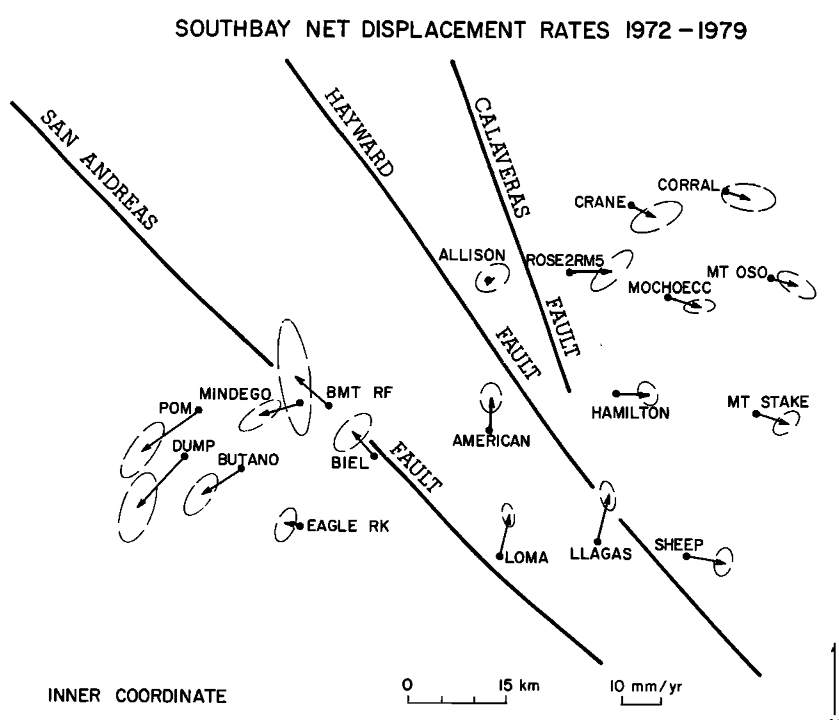

Fig. 6. Vector displacement diagram for the inner coordinate solution. Error ellipses are drawn at the 95% confidence level.

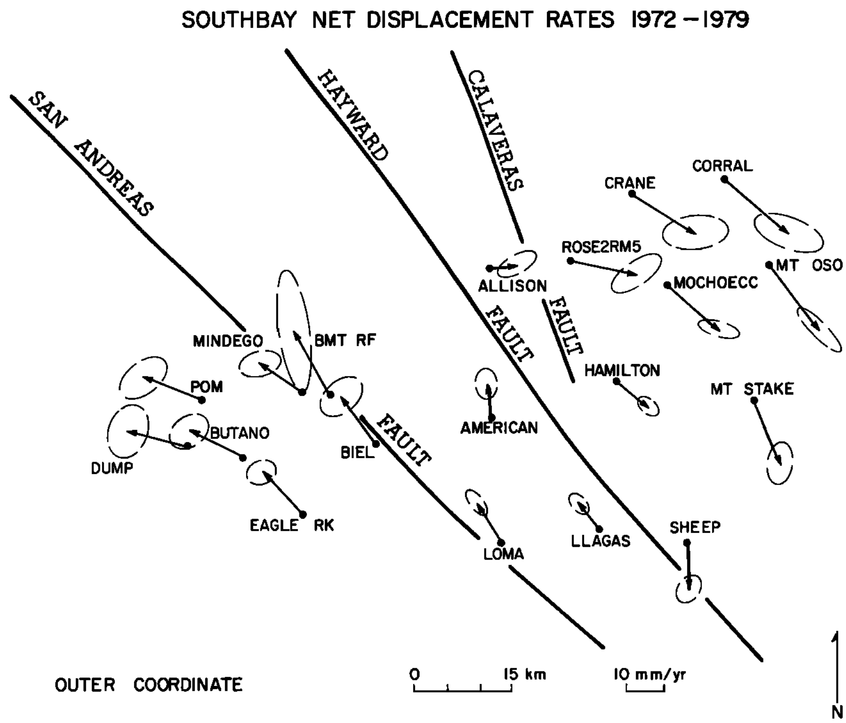

Fig. 7. Vector displacement diagram for an outer coordinate solution. Displacements perpendicular to N35°W have been minimized. Error ellipses are drawn at the 95% confidence level.

and 3*d* can be derived from any of the special solutions in Figures 2*a*, 2*b*, 2*c*, 3*a*, 3*b*, or 3*c* by a similarity transformation [*Brunner,* 1979; *Welsch,* 1979]. An outer coordinate solution with any preferred azimuth can likewise by obtained by a similarity transformation of a special solution. The details of both transformations are given in the appendix.

DISCUSSION

The expected deformation pattern along a strike slip fault is basically simple shear, while the inner coordinate solution is a pure shear solution [see, e.g., *Love,* 1944, p. 33]. It is well known that these two deformation fields differ only by a rigid

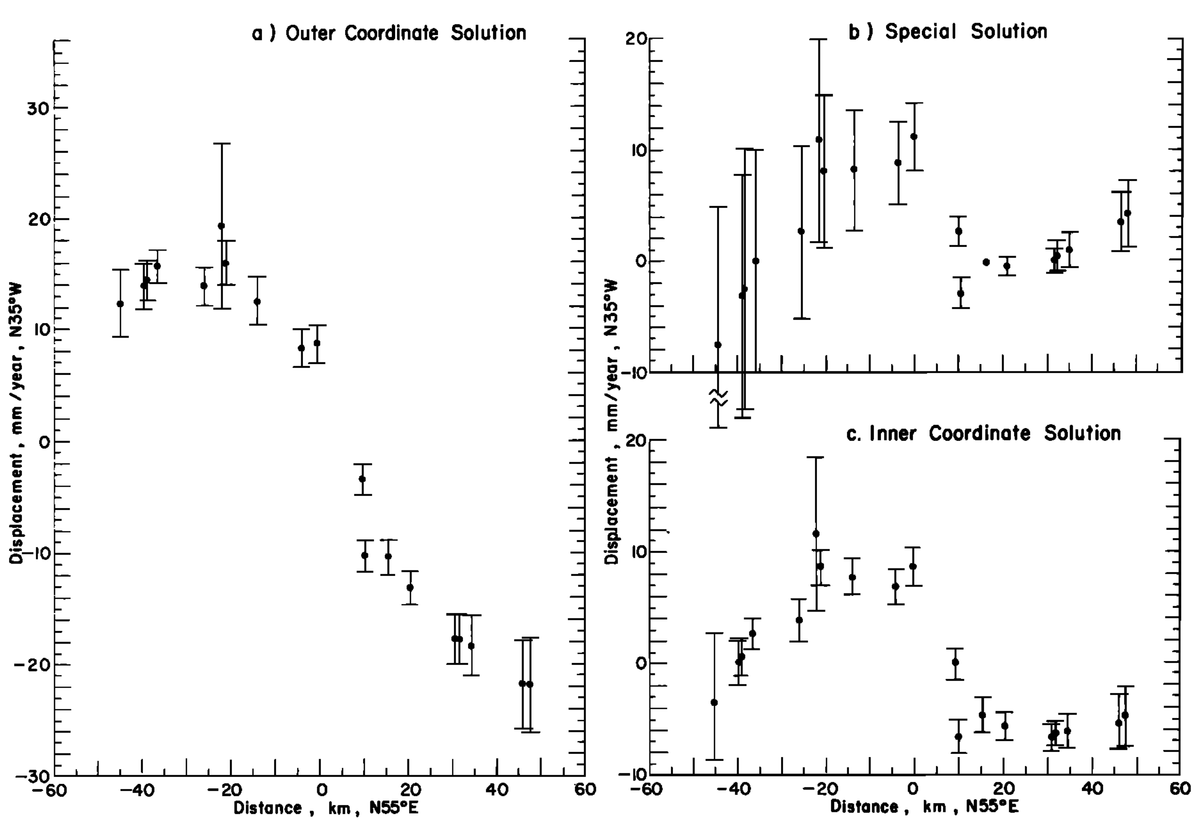

Fig. 8. The displacements parallel to the main trend (N35°W) of the faults are plotted as a function of the station position along the perpendicular direction (N55°E). Error bars indicate plus and minus one standard deviation.

TABLE 1. Statistics From Three Adjustments

	Special Solution	Inner Coordinate Solution	Outer Coordinate Solution
$\sum u_k$, mm	−376.05	0.002	0.002
$\sum v_k$, mm	163.71	−0.002	0.000
$\sum u_k^2$, mm²	8245.6	1323.6	541.9
$\sum v_k^2$, mm²	1616.9	1646.2	3835.1
$\sum(u_k^2 + v_k^2)$, mm²	9862.5	2969.8	4377.0
$\frac{\sum (v_k x_k - u_k y_k)}{\sum (x_k^2 + y_k^2)}$, μrad	0.165	0.0005	−0.172
$\frac{\sum - u_k y_k}{\sum y_k^2}$, μrad	0.340	0.175	0.002

body rotation and internal observations cannot resolve rigid body motion of the entire network. The difference between the various solutions can be critical in interpreting the data, as the following example will illustrate.

One of the most interesting parameters that can be inferred from geodetic networks along the San Andreas fault system (or any strike slip plate boundary) is the relative motion of the two sides. This relative motion is determined by comparing the displacements of stations on opposite sides of the fault or along a line perpendicular to the plate boundary. Such relative motion involves a rotation of the whole network, and consequently, the relative motion which is inferred from the data will depend critically on how the rotation of the whole network is treated. The effect can be illustrated with the network shown in Figure 4. The line lengths were measured periodically between 1972 and 1980. A linear least squares fit to all of the observations of a single line as a function of time was carried out to obtain the average rate of change for each line in Figure 4. These rates were then adjusted by three different methods. Displacement rate vectors for the three adjustments are given in Figures 5–7. Finally, the displacement parallel to the San Andreas fault system (N35°W) was plotted as a function of the distance normal to the fault system (N55°E) in Figure 8. In the first solution, station Hamilton was fixed and station Rose2RM5 was constrained to move along the line connecting it to Hamilton. No error estimate is obtained for Hamilton, of course, since it is fixed. A more serious problem is that any motion of Rose2RM5 perpendicular to the line Hamilton-Rose2RM5 results in apparent motion across the fault, since the entire network is required to rotate to accommodate such a motion of Rose2RM5. A further problem with the special solution is evident in Figure 8. The error ellipses in Figure 5 and the error bars in Figures 8*b* give the error in displacement relative to the fixed station. Since the fixed station displacement is less well determined than the center of mass, the error estimates are larger for Figures 5 and 8*b* than for Figures 6, 7, 8*a* and 8*c*. Next, the special solution was transformed to an inner coordinate solution (Figure 6). Here the entire network is allowed to rotate to a configuration that minimizes the lengths of the displacement vectors. It is apparent from Figure 6 that motion across the fault has been reduced by displacing the northern stations toward the fault and the southern stations away from the fault. Finally, the special solution was transformed to an outer coordinate solution with the azimuth N35°W preferred (Figure 7). This solution of the network finds the rotation which minimizes only the component of displacement normal to the fault rather than both components. The differences between the three solutions are evident in Figure 8. Figures 8*b* and 8*c* both imply significant amounts of left lateral shear, and both seriously underestimate the overall displacement across the network. In fact, for the special solution, Figure 8*b*, the relative displacement across the entire network appears to be left lateral. For the inner coordinate solution the relative displacement across the network is inferred to be about 1 mm/yr, while for the outer coordinate solution it is inferred to be about 36 mm/yr, a value consistent with other estimates of the plate motion rate [*Atwater and Molnar*, 1973; *Minster and Jordan*, 1978, *Thatcher*, 1979].

Some statistics of the three solutions are given in Table 1. As expected, the center of mass of all the stations is stationary for the inner and outer coordinate solutions. The outer coordinate solution has the smallest value for the sum of the squares of the u components of displacement, and the inner coordinate solution has the smallest value for the sum of the squares of both the u components and the v components. Finally, the rotation is zero only for the inner coordinate solution. The special solution has significant counter clockwise rotation while the outer coordinate solution has significant clockwise rotation, consistent with right lateral shear.

APPENDIX

Brunner [1979] has given an English language discussion of the tranformation of a special solution into an inner coordinate solution. I will review this transformation and then show that a very simple modification of the procedure gives the outer coordinate solution.

As a starting point, assume that we have a special solution $\mathbf{U}_s$ and its associated variance-covariance matrix $\mathbf{Q}_s$, explicitly.

$$\mathbf{U}_s^T = [u_1, v_1, u_2, \cdots, u_n, v_n] \tag{A1}$$

where u_k, v_k are the components of displacements of the kth station and superscript T indicates the transpose. We wish to obtain an inner coordinate solution $\mathbf{U}_i$. $\mathbf{U}_i$ must be obtained from $\mathbf{U}_s$ by a rigid body motion; consequently, we can write

$$\mathbf{U}_i = \mathbf{U}_s + \mathbf{Gt} \tag{A2}$$

$\mathbf{G}$ is a constant matrix which depends only on the geometry of the network; $\mathbf{t}$ is an unknown vector which contains information about the rigid body motion. We take

$$\mathbf{t} = \begin{bmatrix} R \\ S \\ \alpha \end{bmatrix}$$

where R is the translation in the x direction, S the translation in the y direction, and α the rotation about the center of the mass. It can be shown the $\mathbf{G}^T$ must have the form

$$\begin{bmatrix} 1 & 0 & 1 & 0 & \cdots & 1 & 0 \\ 0 & 1 & 0 & 1 & \cdots & 0 & 1 \\ y_1 & -x_1 & y_2 & -x_2 & \cdots & y_n & -x_n \end{bmatrix}$$

where the x_k, y_k are the coordinates of the kth station. For reasons which will be clear shortly, we instead take

$$\mathbf{G}^T = \begin{bmatrix} 1/\sqrt{n} & 0 & 1/\sqrt{n} & \cdots & 1/\sqrt{n} & 0 \\ 0 & 1/\sqrt{n} & 0 & \cdots & 0 & 1/\sqrt{n} \\ y_1/D & -x_1/D & y_2/D & \cdots & y_n/D & -x_n/D \end{bmatrix} \tag{A3}$$

where

$$D = \left[\sum (x_k^2 + y_k^2) \right]^{1/2}$$

and x_k, y_k must be measured from the center of mass so

$$\sum x_k = \sum y_k = 0$$

There are a number of ways of characterizing the inner coordinate solution. A convenient one is as follows: the inner coordinate solution is that solution for which the sum of the squares of displacements is minimized. We use this condition to solve (A2) for **t**. That is, we seek the value of **t** that will minimize $\mathbf{U}_i$. Standard least squares techniques [*Bomford*, 1971, p. 630] at once give

$$\mathbf{t} = -(\mathbf{G}^T\mathbf{G})^{-1}\mathbf{G}^T\mathbf{U}_s \tag{A4}$$

Because of our choice of **G**, $\mathbf{G}^T\mathbf{G}$ is the identity matrix, and consequently,

$$\mathbf{t} = -\mathbf{G}^T\mathbf{U}_s \tag{A5}$$

Now substitute (A5) into (A2) to obtain

$$\mathbf{U}_i = (\mathbf{I} - \mathbf{G}\mathbf{G}^T)\mathbf{U}_s \tag{A6}$$

This is a standard expression for transforming a special solution into an inner coordinate solution [*Brunner*, 1979]. The variance-covariance matrix of $\mathbf{U}_i$ is

$$\mathbf{Q}_i = (\mathbf{I} - \mathbf{G}\mathbf{G}^T)\mathbf{Q}_s(\mathbf{I} - \mathbf{G}\mathbf{G}^T)^T \tag{A7}$$

We are now ready to derive the outer coordinate solution, $\mathbf{U}_0$. For convenience, take the preferred direction to lie along the y axis. This can always be arranged by a suitable rotation of the coordinate system. Just as in the inner coordinate solution we must have

$$\mathbf{U}_0 = \mathbf{U}_s + \mathbf{H}\mathbf{t} \tag{A8}$$

where **t** is the same as before but **H** is **G** with a slightly different normalization:

$$\mathbf{H}^T = \begin{bmatrix} 1/\sqrt{n} & 0 & \cdots & 0 \\ 0 & 1/\sqrt{n} & \cdots & 1/\sqrt{n} \\ y_1/E & -x_1/E & \cdots & -x_n/E \end{bmatrix} \tag{A9}$$

where

$$E = \left(\sum y_k^2\right)^{1/2}$$

A condition of the form (A8) is required if $\mathbf{U}_0$ is to differ from $\mathbf{U}_s$ by only rigid body motions. We cannot use (A8) to find the value of **t**, however, or we will end up with an inner coordinate solution. Instead of minimizing the squares of all of the displacements we want to minimize only their x component. We can accomplish this by writing

$$\mathbf{U}_t = \mathbf{U}_s + \mathbf{K}\mathbf{t} \tag{A10}$$

where

$$\mathbf{K}^T = \begin{bmatrix} 1/\sqrt{n} & 0 & 1/\sqrt{n} & 0 & \cdots & 1/\sqrt{n} & 0 \\ 0 & 1/\sqrt{n} & 0 & 1/\sqrt{n} & \cdots & 0 & 1/\sqrt{n} \\ y_1/E & 0 & y_2/E & 0 & \cdots & y_n/E & 0 \end{bmatrix} \tag{A11}$$

E is the same as for (A9). It is clear that if we solve (A10) by least squares for **t**, we will obtain the value of α that minimizes the squares of the u component of displacement but not the v component. Solving (A10) by least squares gives

$$\mathbf{t} = -(\mathbf{K}^T\mathbf{K})\mathbf{K}^T\mathbf{U}_s = -\mathbf{K}^T\mathbf{U}_s \tag{A12}$$

Now substitute (A12) into (A8) to obtain the desired outer coordinate solution:

$$\mathbf{U}_0 = (\mathbf{I} - \mathbf{H}\mathbf{K}^T)\mathbf{U}_s \tag{A13}$$

Its associated variance-covariance matrix is

$$\mathbf{Q}_0 = (\mathbf{I} - \mathbf{H}\mathbf{K}^T)\mathbf{Q}_s(\mathbf{I} - \mathbf{H}\mathbf{K}^T)^T \tag{A14}$$

In deriving the rigid body translation and rotation vector **t** we did not include the weight matrix of the special solution used:

$$\mathbf{P} = \mathbf{Q}_s^{-1}$$

This omission was intentional. We found the rotation-translation which gives the minimum length vectors. That is, $\mathbf{U}_i$ is such that (A2) is satisfied and that $\mathbf{U}_i^T\mathbf{U}_i$ is minimized. Inclusion of the weight matrix **P** would result in satisfying (A2) and minimizing $\mathbf{U}_i^T\mathbf{P}\mathbf{U}_i$. The $\mathbf{U}_i$ obtained would then depend on the special solution used in deriving it; it might be of interest in some applications, but it is not as general a result as the one obtained above. *Brunner* [1979] has shown that $\mathbf{U}_i$ is independent of the special solution from which it is derived. $\mathbf{U}_0$ is of course not unique, since it depends on the preferred azimuth.

Acknowledgment. I thank Walter Welsch for placing my understanding of adjustment theory on a much firmer base.

REFERENCES

Atwater, T., and P. Molnar, Relative motion of the Pacific and North American plates deduced from sea floor spreading in the Atlantic, Indian and South Pacific oceans, Proceedings of the Conference on Tectonic Problems of the San Andreas Fault System, *Stanford Univ. Publ. Geol. Sci., 13*, 136–138, 1973.

Bomford, G., *Geodesy*, 731 pp., Oxford University Press, London, 1971.

Brunner, F. K., On the analysis of geodetic networks for the determination of the incremental strain tensor, *Surv. Rev. Gt. Brit., 25*(192), 56–67, 1979.

Love, A. E. H., *A Treatise on the Mathematical Theory of Elasticity*, Dover, New York, 1944.

Minster, J. B., and T. H. Jordan, Present-day plate motions, *J. Geophys. Res., 83*(B11), 5331–5354, 1978.

Thatcher, W., Systematic inversion of geodetic data in central California, *J. Geophys. Res., 85*(B5), 2283–2296, 1979.

Welsch, W., A review of the adjustment of free networks, *Surv. Rev. Gt. Brit., 25*(194), 67–180, 1979.

(Received September 29, 1980;
revised January 20, 1981;
accepted February 23, 1981.)